THESIS FOR THE DEGREE OF LICENTIATE OF ENGINEERING

Optimal control methods in charge- and trip-planning for electric vehicles

Lorenzo Montalto

Department of Electrical Engineering
Chalmers University of Technology
Gothenburg, Sweden, 2026

Optimal control methods in charge- and trip-planning for electric vehicles

Lorenzo Montalto

Acknowledgements, dedications, and similar personal statements in this thesis, reflect the author's own views.

© Lorenzo Montalto 2026 except where otherwise stated.

Department of Electrical Engineering
Chalmers University of Technology
SE-412 96 Gothenburg, Sweden
Phone: +46 (0)31 772 1000

Cover:
Illustration of an electric vehicle charging at a charging station.

Printed by Chalmers Digital Printing
Gothenburg, Sweden, March 2026

Optimal control methods in charge- and trip-planning for electric vehicles

Lorenzo Montalto
Department of Electrical Engineering
Chalmers University of Technology

Abstract

The transport sector is a major contributor to global greenhouse gas emissions, prompting increasingly stringent regulations and accelerating the transition toward electric mobility. Although electric vehicles (EVs) offer significant potential for emission reduction, their large-scale adoption is still hindered by range anxiety, i.e. the fear of the battery running out before a charging station is reached. Intelligent charge- and trip-planning (ICTP) is a way to address range anxiety by optimizing the charging station selection, the vehicle's energy consumption, the battery thermal management, and the charging process. However, the resulting problems are typically large-scale, nonlinear, and mixed-integer, which makes them computationally challenging to solve. This thesis develops optimal control methods to solve the ICTP problem in a computationally efficient way, to allow real-time onboard implementation.

First, the computational tractability of the ICTP problem is improved through tailored warm-start strategies and the relaxation of binary decision variables, enabling the use of faster continuous solvers and achieving substantial reductions in computation time. Second, a semi-analytical optimal control solver based on Pontryagin's Maximum Principle is developed for EV charging optimization. The solver yields explicit control laws and its low computation time allows for real-time embedded implementation. Finally, a nonlinear optimal control framework for mission planning of long-range solar-powered EVs is proposed, enabling the joint optimization of trip time and energy management under spatio-temporal constraints. The method was tested on a solar-powered vehicle racing across the Australian Outback.

Keywords: Optimal Control, Electrical Vehicles, Optimization, Pontryagin's Maximum Principle, Trip-planning, Charge-planning.

Alla mia famiglia.

List of Publications

This thesis is based on the following publications:

[A] **Lorenzo Montalto**, Nikolce Murgovski, Jonas Fredriksson, "Computationally efficient algorithm for optimal battery preconditioning and charging of electric vehicles". *2024 IEEE 27th International Conference on Intelligent Transportation Systems (ITSC)*, Edmonton, AB, Canada, 2024.

[B] **Lorenzo Montalto**, Nikolce Murgovski, Jonas Fredriksson, "Electrical vehicles charging: an optimal control approach via Pontryagin's Maximum Principle". *2025 IEEE 28th International Conference on Intelligent Transportation Systems (ITSC)*, Gold Coast, QLD, Australia, 2025.

[C] **Lorenzo Montalto**, Nikolce Murgovski, Timothy Jarebrant, "Optimal energy management under spatio-temporal constraints: an application to solar-powered vehicles". Under review in *Control Engineering Practice*, Elsevier, 2026.

Contents

Acknowledgments

First and foremost, I would like to thank my supervisors Nikolce and Jonas for their guidance, patience, and for creating a safe environment for me to experiment, fail and learn. This thesis would not exist without you. I would also like to thank the Swedish Electromobility Center for funding this project.

Thank you to the people of the department, who have all contributed to provide laughter and good vibes during long days at the office. Kilian and Gabriel, for making sure the office is never too serious; Rita, for being my all-knowing unofficial guide when I started; Rémi, for your help during my master's thesis and for our afternoons at Språkcaféet; Attila, for our spontaneous trip to Lappland; Alvin, Ying, Sabino, Nanami, Yara, for our climbing sessions; Kristian, Adam, Chiara, Filip, Isac, Erik, Daniel, Lasse, Zhitao, André, Orlando, Mattia, Godwin, Ahmet, Martina, Francesco, Mohamed and Karthik, for proving that office jobs do not need to be boring.

Thank you to my friends in Gothenburg outside of the department. Aws, for being one of my closest friend throughout my years in Sweden. The guys from Havets Drottning: Deco, Nico, Viktor and Cedrik, for allowing me to share my love for music with dear friends. Zoe, Andreas, Thanos, Eleni and Natalia, for being a reliable source of good memories.

Thank you to my friends back in Turin for coming to Gothenburg to visit me and for being a daily part of my life despite the distance: Fede, Rick, Ste, Vito, Dani, Mauro, Gian, Murru, Bafio and Ema.

A huge thank you to my family, who supported and loved me every single day of my life. Grazie mamma, papà ed Ele.

Thank you to the Källén family for being wonderful people who welcomed me as one of their own from the very first time we met.

Finally, thank you, Julia. Sharing this journey with you is a luxury that I am grateful for and I look forward to its second half by your side.

Acronyms

BWSC:	Bridgestone World Solar Challenge
DS:	Dynamical System

EV:	Electric Vehicle
GHG:	Greenhouse gas
HVCH:	High Voltage Coolant Heater
HP:	Heat Pump
HVAC:	Heating, Ventilation and Air Conditioning
ICEV:	Internal Combustion Engine Vehicle
ICTP:	Intelligent Charge- and Trip-Planning
Li-ion:	Lithium-ion
LTS:	Location-Triggered Stop
ML:	Machine Learning
MPC:	Model Predictive Control
NRM:	Newton-Raphson Method
NN:	Neural Network
OCP:	Optimal Control Problem
PMP:	Pontryagin's Maximum Principle
RK4:	4th order Runge-Kutta
SoC:	State of Charge
TTS:	Time-Triggered Stop

Part I

Overview

CHAPTER 1

Introduction

1.1 Motivation: climate neutrality and electric vehicles

One of the main challenges that define our time is climate change. According to the European Climate Law of 2021 [1], Europe aims to be climate neutral by 2050, meaning that it aims to reduce greenhouse gas (GHG) emissions caused by human activities [2]. This goal can be considered a consequence of the Paris Agreement [3], signed in 2015 by 195 Parties at the UN Climate Change Conference in Paris, France. The goal of the agreement is to hold the increase in global average temperature to well below 2°C above pre-industrial levels and pursue efforts to limit said increase to 1.5°C above pre-industrial levels. If this sounds like an ambitious goal, that would be because it is. In fact, 2024 was the first year with an average temperature clearly exceeding 1.5°C above pre-industrial levels [4]. This paints a picture of a critical situation that needs to be addressed as soon as possible.

Given the urgency of the situation, it seems reasonable to act on the sectors which contribute the most to this worrying trend. When it comes to CO2

emissions by sector, the transport sector stands out as one of the most critical [5], which is why it is not hard to find recent research focused on finding ways to make it more sustainable [6]. A way to address this has been to promote the use of electric vehicles (EVs) [7]. While it is true that, under certain conditions, EVs are greener than internal combustion engine vehicles (ICEVs) [8], there are some issues that discourage their adoption. One such issue is what is known in the literature as *range anxiety* [9], that is, the fear of the battery running out before reaching the destination. Range anxiety is further exacerbated by the fact that charging stations are less common than refueling stations [10]. Another issue is that recharging is generally much more time-consuming than refueling, which also introduces safety issues, as having to spend a long time at a charging station at night might be uncomfortable for some people, which might be especially true for women [11]. All these factors make EVs less flexible and appealing than ICEVs. Therefore, to effectively promote the use of EVs, these issues need to be addressed.

Since EVs have a shorter range than ICEVs, an intuitive hardware-side solution to range anxiety would be to increase the battery's size. In fact, due to its impact on weight and production costs, optimizing the battery's size is a crucial problem that is well explored in the literature [12, 13]. To avoid increasing production costs by having a bigger battery, one can instead focus on improving the vehicle's energy efficiency. Lithium-ion (Li-ion) batteries, commonly used in EVs, operate suboptimally when their temperature is too low (less than 0°C) or too high (above 35°C) [14]. One way to address this is battery thermal management (BTM), which consists in actively controlling the battery's temperature so that it lies within its optimal range. Another strategy for improving the EV's efficiency is by optimizing its driving profile, such that it is guaranteed that it reaches the destination while optimizing energy consumption. This is known as eco-driving [15]. BTM and eco-driving can be integrated into a larger scheme to address range anxiety, which also includes the optimization of the charging process and of the charging stations selection. This is known as intelligent charge- and trip-planning (ICTP) and is what this thesis focuses on.

1.2 Intelligent charge- and trip-planning

ICTP is the coordinated planning and optimization of several aspects of EV operation, including BTM, the vehicle's driving profile, the selection of charging stations, and the charging process itself. The optimization of the charging process typically involves balancing conflicting objectives, such as minimizing charging time while simultaneously reducing economic cost, which may vary depending on charging power, electricity prices, and location of the charging station. Similarly, optimizing the driving profile aims at minimizing energy consumption while also ensuring that the battery temperature is maintained within its optimal operating range, particularly prior to reaching the next charging station, to enable efficient and fast charging. These decisions are tightly interconnected. For instance, driving behavior affects both energy consumption and battery temperature, which in turn influence the available driving range and the efficiency of subsequent charging events. As a result, ICTP should be formulated as an optimal control problem (OCP) in which the states, control inputs, and discrete decisions must be optimized jointly while guaranteeing that the destination is reached without battery depletion. Due to the presence of nonlinear dynamics, operational constraints, and discrete choices such as charging station selection, the resulting OCP is typically large-scale, non-convex, and potentially mixed-integer. These characteristics significantly increase the computational complexity of the problem. It is therefore important to address these computational challenges so that the ICTP problem can be solved efficiently.

A common approach to handling integer decision variables in eco-driving problems is the use of relaxation techniques [16]. By relaxing integer constraints into continuous ones, the resulting problem can be solved efficiently with only minor modifications to the original formulation, yielding solutions that are computationally inexpensive and have good practical performance. However, for non-convex problems, relaxation-based methods might converge to locally optimal solutions, depending heavily on the initial guesses for the relaxed integer variables. A local optimum is a solution that minimizes the cost function in a certain interval but is not necessarily the minimum of the function over its entire domain. An alternative approach that has been used for routing and eco-driving problems in electric vehicles is Dynamic Programming (DP) [17–19], a technique that relies on a *divide and conquer* principle, which consists of solving a problem by breaking it into smaller subproblems and

combining their solutions. DP is capable of computing globally optimal solutions for fully integer problems. However, in mixed-integer problems involving continuous variables, DP does not, in general, solve the original problem directly, but rather an approximated version in which continuous states and control inputs are quantized. This quantization introduces an approximation whose quality depends on how finely the variables are quantized. Moreover, the computational complexity of DP grows exponentially with the size of the problem and the number of quantized points, a phenomenon known as *curse of dimensionality*, making its original formulation intractable in reality. An alternative to DP to solve the routing problem for EVs is machine learning (ML) [20–22]. ML makes it possible to train models to describe complicated systems without the need to understand how they work. This is the reason why these models are often referred to as *black boxes*, meaning that the relationship between the input and the output is unknown to the user. The drawback of ML methods is that a lot of data is usually needed to train a model and said model is rarely interpretable. This makes these methods not suitable in applications where guarantees of stability or constraint satisfaction might be needed.

Within model-based approaches, optimal control techniques play a central role, as they guarantee that the obtained solution optimizes some given metric. A classic model-based optimal control framework is Model Predictive Control (MPC), which has been successfully applied to solve charging problems [23, 24] and energy management problems [25] for EVs. MPC relies on a model of the system to predict the state evolution and plan the control accordingly. The key aspect that makes MPC so widely used is that it makes it possible to easily deal with constraints in the problem, as they are explicitly embedded in the problem formulation. A potential drawback of MPC is the need to numerically solve an optimization problem at each sampling step, which might make it computationally heavy, depending on the size of the problem. In contrast to this, an analytical optimal control method is Pontryagin's Maximum Principle (PMP) [26], a core result in optimal control theory which provides necessary conditions for optimality, which become sufficient under certain appropriate convexity conditions. PMP-based methods have been successfully applied to thermal and energy management problems and routing in EVs [27–29]. PMP-based methods allow for the retrieval of an analytical (or semi-analytical) solution to an optimization problem, revealing the underlying structure of the

optimal solution and how each variable and parameter affect it. The derivation of the analytical expressions for the optimal control laws can be shifted to an offline phase that is executed only once, potentially reducing the overall computational burden needed to solve the problem. The primary limitation of this approach is that their reliance on analytically derived optimal control laws requires problem-specific formulation and implementation, meaning that any change in the model or in the problem formulation usually results in some change in the algorithm, or at least in a need to recompute the optimal expressions. Moreover, it is not always guaranteed that analytical expressions for the optimal control inputs are attainable. However, if the problem is well-defined and its formulation remains consistent, building the solver around it makes it possible to exploit its specific structure and properties.

Based on the reviewed literature, a clear pattern emerges: significant progress has been made in energy management, speed optimization, and trip-level planning for EVs, yet these components are typically addressed either in isolation or within hierarchical architectures that decompose the overall problem.

Several works, such as [30] and [31], adopt a multi-layer structure, where trip planning, energy management, and speed control are solved as separate subproblems using different techniques (e.g., DP and nonlinear MPC). Although this decomposition supports real-time feasibility, it generally sacrifices global optimality and requires coordination mechanisms between layers. Moreover, the use of DP or large-scale nonlinear optimization can lead to substantial computational complexity.

From a PMP perspective, works such as [32], [33], and [34] demonstrate that analytical optimal control can significantly reduce online computation. However, these approaches typically target single subsystems (e.g., torque split, speed trajectory, or BTM) and often rely on approximations to remain computationally tractable. The integration of multiple physical domains, such as trip planning, charging decisions, battery state-of-charge dynamics, and thermal constraints, into a single, structure-exploiting PMP-based framework remains largely unexplored.

Importantly, across the reviewed literature, three common limitations can be identified:

1. Fragmented problem formulations: Trip planning, speed optimization, charging decisions, and thermal management are usually treated separately or hierarchically, rather than as a single unified optimal control

problem.

2. Computational scalability challenges: DP-based and nonlinear MPC-based solutions suffer from the curse of dimensionality or repeated online optimization, limiting their applicability to embedded hardware.

3. Limited exploitation of analytical structure at the system level: While PMP has been successfully applied to subsystem-level problems, there is a lack of systematic methodologies for deriving computationally efficient, semi-analytical solvers for integrated charge- and trip-planning problems with realistic constraints.

The goal of this thesis is to move in the direction of filling this gap.

1.3 Thesis contributions

This thesis investigates model-based optimal control algorithms for solving the ICTP problem for electric vehicles (EVs). Particular emphasis is placed on ensuring that the proposed methods are computationally efficient and suitable for practical implementation. Two levels of computational performance are distinguished: computational viability and real-time implementability. An algorithm is considered computationally viable if the associated optimization problem can be solved in approximately one minute on the intended hardware platform. Such algorithms are suitable for offline planning or receding-horizon strategies with relatively long update intervals, but they are not necessarily intended for execution within strict online timing constraints. Real-time implementability constitutes a more stringent requirement. It refers to the ability of an algorithm to consistently compute a feasible and reliable solution within the short time frame imposed by an online control system, typically on the order of one second or less. This requirement is particularly relevant for deployment on vehicular electronic control units (ECUs), which are characterized by limited computational resources and memory capacity. By definition, real-time implementability implies computational viability, whereas the converse does not necessarily hold.

More specifically, the contributions of this thesis can be grouped into two categories based on their time scale and computational objectives.

- The trajectory planning problem of a solar-powered electric vehicle over long time horizons, on the order of a few thousands of kilometers,

is solved through an optimal control framework. The driving profile is obtained by solving a minimum-time optimal control problem that accounts for nonstandard spatio-temporal constraints. These include location-based constraints, such as charging stops at fixed stations with free arrival times, and time-based constraints, such as driving breaks occurring at predetermined times but unknown locations. The resulting formulation guarantees constraint satisfaction and differentiability while minimizing total travel time. This contribution is intended for offline analysis and performance assessment, providing optimal trajectories that can serve as a benchmark or as guidance for a human driver, rather than for real-time implementation.

- The computational efficiency of optimization-based methods for EV charging and energy management problems is improved. In particular, the computational viability of an existing mixed-integer ICTP solver is improved by relaxing its integer variables and designing an initialization strategy that generates initial guesses close to the optimal solution, thereby facilitating convergence and reducing execution time. In addition, the EV charging optimization problem is addressed using a custom PMP-based solver, which enables the computation of a semi-analytical solution and shifts a significant portion of the computational effort offline, making the approach suitable for real-time applications.

1.4 Thesis outline

This thesis is structured in two main parts. Part I, comprising six chapters, serves as an introduction to the ICTP problem, its mathematical formulation, and the optimization tools used to solve it. Part II contains the papers upon which the thesis is based. The remainder of this section outlines the content of Part I.

Chapter 2 presents the mathematical modeling of the different domains involved in the analyzed system and formulates the continuous-time OCP addressed in the thesis. It also introduces the corresponding discretized formulation required for digital implementation. Chapter 3 describes the optimization tools and methods employed throughout the thesis to solve the defined OCP. Chapter 4 explains how all the previously defined elements are combined to develop the solutions and the methods proposed in the thesis. Chapter 5 pro-

vides a concise summary of the papers included in the thesis. Finally, Chapter 6 offers some concluding remarks, discusses and interprets the main results, and outlines directions for future research.

CHAPTER 2

Mathematical modeling and problem formulation

2.1 Mathematical modeling

This section provides an overview on how the systems in Paper A-C are modeled mathematically.

Dynamical system

In Paper A-C, the system to be controlled is modeled as a dynamical system, meaning that its evolution over time (or over some other independent variable) is described by a set of differential equations

$$\dot{\mathbf{x}}(t) = f_x(\mathbf{x}, \mathbf{u}) \tag{2.1}$$

where $\mathbf{x}$ is the state vector, $\mathbf{u}$ is the control vector and f_x depends on the specific system that is being modeled. States and control inputs are often bounded in some feasible sets, meaning that they cannot take on any value.

This is formalized as

$$\mathbf{x} \in \mathcal{X} \subseteq \mathbb{R}^{n_x} \tag{2.2a}$$

$$\mathbf{u} \in \mathcal{U} \subseteq \mathbb{R}^{n_u} \tag{2.2b}$$

where $\mathcal{X}$ and $\mathcal{U}$ are, respectively, the set of feasible states and the set of feasible control inputs, while n_x and n_u are, respectively, the number of state variables and the number of control inputs.

In Paper A-C, the analyzed dynamical system is a vehicle with the following states and control inputs

$$\mathbf{x}(t) = \begin{bmatrix} T_\mathrm{b}(t) & \mathrm{SoC}(t) & \tau(t) & s(t) & E_\mathrm{k}(t) \end{bmatrix}^\intercal \tag{2.3}$$

$$\mathbf{u}(t) = \begin{bmatrix} P_\mathrm{b}(t) & P_\mathrm{hvch}(t) & P_\mathrm{hp}(t) & P_\mathrm{hvac}(t) & a(t) \end{bmatrix}^\intercal \tag{2.4}$$

where T_b is the battery temperature, SoC is the state of charge, τ is the driving time, s is the location of the vehicle, E_k is the kinetic energy, P_b is the battery power, P_hvch is the high voltage coolant heater (HVCH) power, P_hp is the heat pump (HP) power, P_hvac is the power for heating, ventilation and air conditioning (HVAC), and a is the acceleration. The function f_x which describes the evolution of these states over time is assumed to be known.

Each paper uses a subset of these states and control inputs, meaning that the formulation with these vectors is the most general.

Thermal modeling

The charging and discharging performance of EVs is greatly affected by their battery temperature [35–37], which makes it vital to maintain it in an optimal range, both to increase vehicle performance and efficiency, but also to prolong battery life [38]. The BTM process of actively controlling the battery temperature to ensure that it is within its optimal range, which is usually around 20°C - 25°C [37, 38], is known as *preconditioning*. The algorithm developed in Paper A generates, through heuristics, an initial guess for the control inputs trajectories needed to perform preconditioning.

In Paper A and B, the state vector includes a thermal state: the battery temperature T_b. To maintain a notation similar to (2.1), the evolution over time of the battery temperature can be summarized as

$$\dot{T}_\mathrm{b}(t) = f_{T_\mathrm{b}}(\mathbf{x}, \mathbf{u}) \tag{2.5}$$

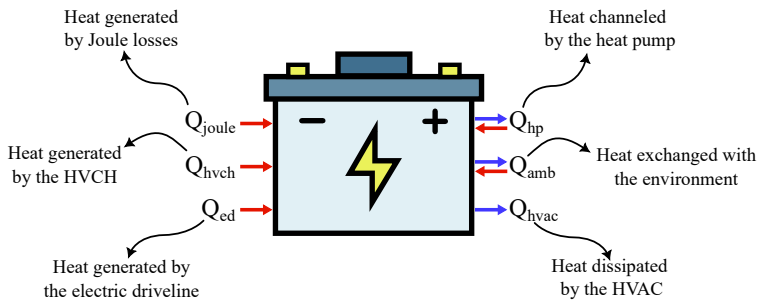

Figure 2.1: Schematic of the thermal modeling of the battery, showing the elements that heat it up (red arrow) and those that cool it down (blue arrow).

where f_{T_b} is assumed to be known. Figure 2.1 shows a schematic representation of all the elements which affect the battery temperature T_b. A red arrow towards the battery indicates something that heats it up, while a blue arrow that goes away from the battery indicates something that cools it down.

The battery temperature T_b can be actively controlled through three control inputs: the HVCH power, the HP power, and the HVAC power. The HVCH and the HVAC are opposite, in the sense that the former is used to heat up the battery while the latter to cool it down. The HP channels heat between the battery and the cabin compartment, meaning that, in principle, it can be used both to heat up the battery and to cool it down. In Paper A and B, the HP is only used to cool down the battery (which, in turn, heats up the cabin compartment).

Aside from active BTM, the battery temperature can also be influenced by other aspects. For instance, Joule heating caused by the current passing through the battery heats it up. The power generated by the electric driveline (also referred to as propulsion power) also generates heat, indicated as Q_ed. Finally, the battery exchanges heat with the environment, meaning that the battery can either lose or gain heat depending on whether it is warmer or colder than the environment.

A more detailed description of (2.5), including all the equations for the thermal elements indicated in Figure 2.1, can be found in Paper A and B.

Electrical modeling

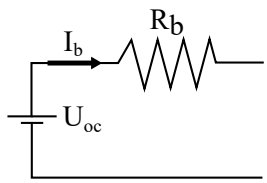

Figure 2.2: Electrical model of the battery.

In Paper A,B, the battery is modeled as the equivalent circuit shown in Figure 2.2, having as single electrical state the state of charge (SoC), which is a measure of the amount of energy in the battery. The internal resistance R_b is a function of the battery temperature T_b, where a higher T_b translates to a lower R_b [39]. The open circuit voltage U_oc is a function of the SoC, where a higher SoC translates to a higher U_oc [40]. Finally, I_b is the battery's internal current. The evolution of the SoC over time can then be summarized as

$$\dot{\mathrm{SoC}}(t) = f_\mathrm{SoC}(\mathbf{x}, \mathbf{u}). \tag{2.6}$$

The details of (2.6), of the relationship between R_b and T_b, and of the relationship between U_oc and SoC can be found in Paper A and B.

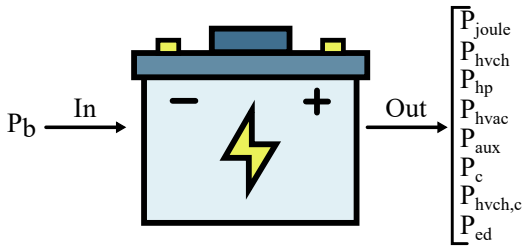

Figure 2.3: Schematic of the battery's power balance.

To ensure that the power provided by the battery does not exceed its internal available chemical power, a power balance constraint is enforced. This is visually represented in Figure 2.3. The term on the left (P_b) is the internal chemical power of the battery. The terms on the right include: the

Joule losses, the power needed for active thermal management (HVCH, HP and HVAC), the power needed for auxiliary devices in the vehicle (e.g., infotainment), the power needed for cabin compartment heating (P_{c}), the portion of the HVCH power used to heat up the cabin compartment ($P_{\mathrm{hvch,c}}$) and, finally, the power needed for the propulsion of the electrical driveline (P_{ed}).

Solar irradiance

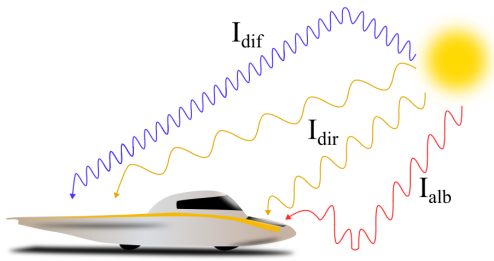

Figure 2.4: Illustration of the different kinds of solar irradiance.

The system analyzed in Paper C is a solar-powered EV, with solar panels both in the front and in the back. To compute the energy that the EV obtains from the sun, three different types of solar irradiance are considered, which can be seen in Figure 2.4.

The main contribution to solar irradiance is from direct sunlight (I_{dir}), which is mostly influenced by the angle of incidence between the Sun's rays and the solar panels. That is, it is maximized if the panels perfectly face the Sun. The second contribution is given by the Sun's rays being scattered by the atmosphere (I_{dif}), while the last one is given by the reflection of the sunlight on the ground (I_{alb}). The details on how all of these elements are computed can be found in Paper C.

Forces acting on the vehicle

Figure 2.5 shows the forces acting on the vehicle for the mission planning problem in Paper C. F_{drag} is the aerodynamic drag, F_{gravity} is the gravitational force, F_{roll} is the force due to rolling resistance, F_{prop} is the force that propels

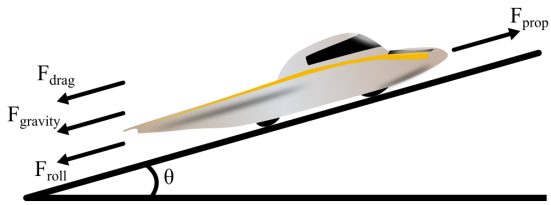

Figure 2.5: Schematics of the forces acting on the solar-powered EV in Paper C.

the vehicle forward, and θ is the slope of the terrain. The details of how all of the forces are computed and handled can be found in Paper C.

2.2 Optimal control problem formulation

In Paper A-C, the control task is solved as an optimal control problem (OCP), which is a subset of control problems whose goal is to find a control trajectory for a dynamical system such that a given cost function is minimized. The dynamical system is described as in (2.1) and the cost function can generally be defined as

$$J = \Psi(\mathbf{x}(t_\mathrm{f})) + \int_0^{t_\mathrm{f}} S(\mathbf{x}, \mathbf{u}) \mathrm{d}t \tag{2.7}$$

where S is known as the *stage cost*, which can be interpreted as the rate of cost for exerting control $\mathbf{u}$ in state $\mathbf{x}$, t_f is the final time, and Ψ is the *final cost*, which can be interpreted as the cost for ending up in state $\mathbf{x}(t_\mathrm{f})$.

A general definition of the ICTP problem solved in Paper A-C, formulated

as a continuous-time OCP, is then given by

$$\min_{\mathbf{x},\mathbf{u},\mathbf{b},t_\mathrm{f}} \; J = \Psi(\mathbf{x}(t_\mathrm{f})) + \int_0^{t_\mathrm{f}} S(\mathbf{x},\mathbf{u})\mathrm{d}t \tag{2.8a}$$

$$\text{s.t.: } \dot{\mathbf{x}}(t) = f_x(\mathbf{x},\mathbf{u}) \tag{2.8b}$$

$$\mathbf{x}(t) \in \mathcal{X},\ \mathbf{u}(t) \in \mathcal{U},\ t \in [0, t_\mathrm{f}] \tag{2.8c}$$

$$t_\mathrm{f} \in [0, T_\mathrm{max}] \tag{2.8d}$$

$$\mathbf{b} \in \{0,1\}^{N_\mathrm{b}} \tag{2.8e}$$

$$\mathbf{h}_\mathrm{b}(\mathbf{x},\mathbf{u},\mathbf{b}) \leq 0 \tag{2.8f}$$

$$\mathbf{x}(0) = \bar{\mathbf{x}}_0,\ \mathbf{x}(t_\mathrm{f}) \in \mathcal{X}_\mathrm{f} \tag{2.8g}$$

where $\mathbf{b}$ is a vector of binary decision variables of length N_b, T_max is the upper bound for the final time, $\mathbf{h}_\mathrm{b}$ is a vector of constraints (either equality or inequality), $\bar{\mathbf{x}}_0$ is some known initial condition, and $\mathcal{X}_\mathrm{f}$ is a known target set for the states.

The vector of binary decision variables $\mathbf{b}$ is used to model binary decisions in the problem. More specifically, in Paper A all charging stations along the trip have a binary variable associated to them, which is equal to 1 if the station is chosen to recharge the vehicle, and equal to 0 otherwise.

Since this problem is in continuous time, it is infinite-dimensional, which might make it hard to solve. Closed-form expressions of the optimal control laws for (2.8) are obtained in Paper B. However, to obtain a numerical solution, the problem has to be discretized so that it can be solved numerically.

2.3 Discretization of an OCP

Different methods can be used to discretize an OCP. In particular, this thesis uses two, which are the ones described in this section.

Forward Euler method

In Paper C, the forward Euler method is used to discretize (2.1). The method is illustrated in Figure 2.6, where $\mathbf{x}(t)$ denotes the continuous-time state trajectory, the red curve represents its discrete-time approximation obtained using the forward Euler scheme, and h denotes the discretization step size. A lower value of h generally yields a more accurate approximation of the

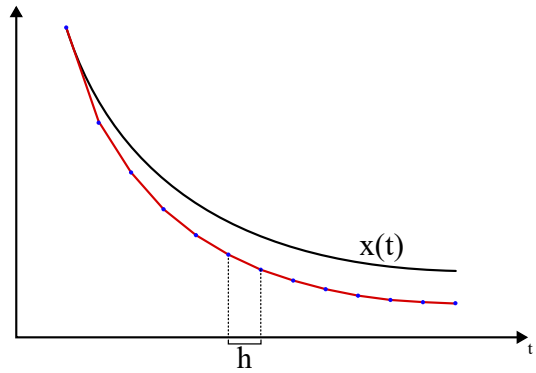

Figure 2.6: Visualization of the forward Euler method.

continuous-time dynamics, at the expense of increased computational complexity due to the larger number of time steps required.

The forward Euler method is the simplest explicit numerical integration scheme and is based on a first-order approximation of the time derivative. Assuming that the time evolution of the state vector $\mathbf{x}$ is governed by (2.1), the method approximates the derivative by a finite difference over a non-infinitesimal time interval, essentially replacing the limit definition of the derivative with a discrete increment in both state and time

$$\frac{\mathrm{d}\mathbf{x}}{\mathrm{d}t} = f_x(\mathbf{x}, \mathbf{u}) \tag{2.9a}$$

$$\Rightarrow \frac{\Delta\mathbf{x}}{\Delta t} \approx f_x(\mathbf{x}, \mathbf{u}) \tag{2.9b}$$

$$\Rightarrow \Delta\mathbf{x} \approx f_x(\mathbf{x}, \mathbf{u}) \cdot \Delta t. \tag{2.9c}$$

If the step size of the discretization is defined as $h = \Delta t$, the discrete-time update for the states is as follows

$$\mathbf{x}_{n+1} = \mathbf{x}_n + \Delta\mathbf{x}_n = \mathbf{x}_n + f_x(\mathbf{x}_n, \mathbf{u}_n) \cdot h. \tag{2.10}$$

The method is simple to implement and computationally efficient, but also not particularly accurate, as shown in Figure 2.6. For this reason, more sophisticated integration methods can be used to discretize a dynamical system.

Runge-Kutta method

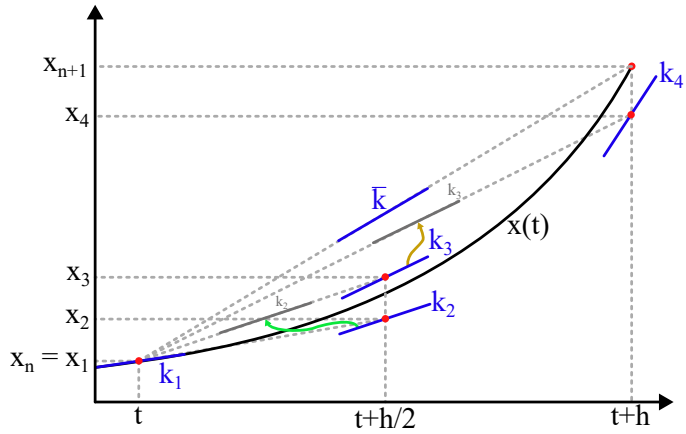

Figure 2.7: Illustration of the 4th order Runge-Kutta method.

In Paper A and B, the Runge-Kutta method is used to discretize (2.1). More specifically, the variant of the method known as 4th order Runge-Kutta (RK4) is used.

The method is illustrated in Figure 2.7, where $\mathbf{x}$ is the function that needs to be discretized, and h is the step size of the discretization, which handles the same trade-off between accuracy and computational complexity as for the Euler method. Assuming $\mathbf{x}_n$ is known and that zero-order hold is used, meaning that the control input u_n is kept constant over the interval $[t, t+h]$, the discrete-time update for the states is as follows

$$\mathbf{x}_{n+1} = \mathbf{x}_n + \frac{h}{6}\left(k_1 + 2k_2 + 2k_3 + k_4\right) \tag{2.11a}$$

$$k_1 = f_x(\mathbf{x}_n, \mathbf{u}_n) \tag{2.11b}$$

$$k_2 = f_x\left(\mathbf{x}_n + \frac{h}{2}k_1, \mathbf{u}_n\right) \tag{2.11c}$$

$$k_3 = f_x\left(\mathbf{x}_n + \frac{h}{2}k_2, \mathbf{u}_n\right) \tag{2.11d}$$

$$k_4 = f_x\left(\mathbf{x}_n + hk_3, \mathbf{u}_n\right) \tag{2.11e}$$

The method is a 4th order one because four slopes are computed to get from one sample of the function to the next one, as opposed to using only one as is done in the much simpler forward Euler method. This makes RK4 more computationally expensive than the forward Euler method but also much more accurate.

2.4 Discretized OCP

If the dynamical system in (2.1) is discretized as per Section 2.3, then the problem in (2.8) has to be discretized as well. Before discretization, the cost function has to be reformulated. Namely, the stage cost is integrated in $[0, t_\mathrm{f}]$, but since t_f is a decision variable, and is therefore not known in advance, the integral can be evaluated only after the problem is solved. The integral is therefore normalized, using the normalized time τ as the integration variable, defined as

$$\tau = \frac{t}{t_\mathrm{f}} \Rightarrow t = t_\mathrm{f}\tau. \tag{2.12}$$

The integral then becomes

$$\int_0^{t_\mathrm{f}} S(\mathbf{x}, \mathbf{u})\mathrm{d}t = t_\mathrm{f} \int_0^1 S(\mathbf{x}, \mathbf{u})\mathrm{d}\tau. \tag{2.13}$$

If the independent variable becomes the normalized time τ, then (2.1) is affected as well, as it should be expressed in terms of τ. Given (2.12), the dynamic equation for the states in normalized time is obtained through the chain rule

$$\frac{\mathrm{d}x}{\mathrm{d}\tau} = \frac{\mathrm{d}x}{\mathrm{d}t} \cdot \frac{\mathrm{d}t}{\mathrm{d}\tau} = f_x(\mathbf{x}, \mathbf{u}) \cdot t_\mathrm{f}. \tag{2.14}$$

Knowing this, it is possible to now discretize the problem as follows

$$\min_{\mathbf{x},\mathbf{u},\mathbf{b},t_\mathrm{f}} \; J = \Psi(\mathbf{x}_N) + t_\mathrm{f} \sum_{k=0}^{N-1} S_\mathrm{d}(\mathbf{x}_n, \mathbf{u}_n) \tag{2.15a}$$

$$\text{s.t.: } \mathbf{x}_{n+1} = t_\mathrm{f} \cdot f_\mathrm{d}(\mathbf{x}_n, \mathbf{u}_n),\ n = 0, \ldots, N-1 \tag{2.15b}$$

$$\mathbf{x}_n \in \mathcal{X},\ \mathbf{u}_n \in \mathcal{U},\ n = 0, \ldots, N-1 \tag{2.15c}$$

$$t_\mathrm{f} \in [0,\, T_\mathrm{max}] \tag{2.15d}$$

$$\mathbf{b} \in \{0,1\}^{N_\mathrm{b}} \tag{2.15e}$$

$$\mathbf{h}_\mathrm{b}(\mathbf{x}, \mathbf{u}, \mathbf{b}) \leq 0 \tag{2.15f}$$

$$\mathbf{x}_0 = \bar{\mathbf{x}}_0,\ \mathbf{x}_N \in \mathcal{X}_\mathrm{f}. \tag{2.15g}$$

where f_d and S_d depend on the specific integration scheme that is used and $\bar{\mathbf{x}}_0$ is a known initial condition for the state. Notice that, while t_f is not known a priori, the number of samples N is known and decided based on the sampling interval h. The problems solved concretely in Paper A-C are different versions of this formulation.

CHAPTER 3

Optimization tools

This chapter introduces the mathematical tools used to solve the OCPs described in 2.8 and 2.15.

3.1 Boundary value problem

A boundary value problem is a differential equation subjected to constraints called boundary conditions. Solving a boundary value problem means finding a solution to the differential equation which also satisfies the boundary conditions. The name refers to the fact that the above-mentioned constraints are specified at the boundary of the domain where the problem is to be solved. The OCP in Paper B is solved as a boundary value problem.

A boundary value problem can, for instance, be defined as

$$\dot{\boldsymbol{\xi}}(t) = f_{\xi}(\boldsymbol{\xi}, \mathbf{u}) \tag{3.1a}$$

$$\boldsymbol{\xi}(t_0) = \boldsymbol{\xi}_0,\ \boldsymbol{\xi}(t_\mathrm{f}) = \boldsymbol{\xi}_\mathrm{f}. \tag{3.1b}$$

where $\boldsymbol{\xi}$ is the extended state vector including both states and costates

$$\boldsymbol{\xi} = [\mathbf{x},\ \boldsymbol{\lambda}]^\intercal. \tag{3.2}$$

The vector of costates $\boldsymbol{\lambda}$ is defined more in details later in section 3.6. The goal is to find the function $\boldsymbol{\xi}(t)$ over the interval $[t_0, t_\mathrm{f}]$ which solves (3.1a) while satisfying (3.1b).

3.2 Shooting method

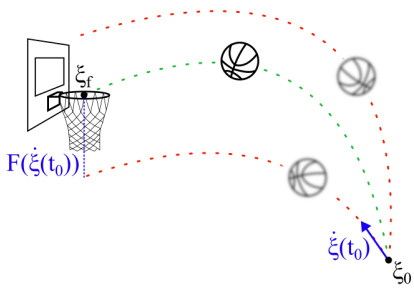

Figure 3.1: Solving a boundary value problem with the single shooting method can be visualized as a basketball shot.

Shooting methods are numerical methods used to solve boundary value problems, as those described in 3.1. The OCPs in Paper A-C are solved numerically through shooting methods. These methods can be differentiated into single and multiple shooting.

Single shooting methods solve a boundary value problem by computing the entire solution at once. As an example, consider the problem in (3.1). The error between the final state $\boldsymbol{\xi}(t_\mathrm{f})$ and the desired one $\boldsymbol{\xi}_\mathrm{f}$ is defined as

$$F(\dot{\boldsymbol{\xi}}(t_0)) = \boldsymbol{\xi}(t_\mathrm{f}) - \boldsymbol{\xi}_\mathrm{f}. \tag{3.3}$$

The reason why F is a function of $\dot{\boldsymbol{\xi}}(t_0)$ is that $\boldsymbol{\xi}(t_\mathrm{f})$ is obtained by integrating (3.1a), starting from a known $\boldsymbol{\xi}_0$ and from an unknown $\dot{\boldsymbol{\xi}}(t_0)$. The goal is then to find $\dot{\boldsymbol{\xi}}(t_0)$ such that $F(\dot{\boldsymbol{\xi}}(t_0)) = 0$, which is essentially a root-finding problem. Single shooting is used in Paper B, where the developed solver reconstructs the solution starting from the known initial and final conditions.

The single shooting method can be illustrated as in Figure 3.1, which also conveys the intuition behind its name. The initial position of the ball, $\boldsymbol{\xi}_0$ (corresponding to the player's location), and the desired terminal position, $\boldsymbol{\xi}_\mathrm{f}$

(the basket), are known. The objective is to determine the appropriate initial velocity $\dot{\boldsymbol{\xi}}(t_0)$ (depicted by the blue arrow in the lower right of the figure), such that the resulting trajectory satisfies the terminal condition (i.e. the ball goes into the basket). Although all three trajectories shown in the figure satisfy (3.1a), the red trajectories correspond to initial velocities for which $F(\dot{\boldsymbol{\xi}}(t_0)) \neq 0$, implying that the terminal constraint is not fulfilled (i.e. the ball misses the basket).

A fundamental limitation of single shooting is its sensitivity to numerical errors. Since the trajectory is computed over the entire interval in a single forward integration, local discretization errors may accumulate and propagate throughout the interval. Moreover, the satisfaction of the terminal condition can only be assessed after the complete trajectory has been computed. To mitigate these issues, one may introduce intermediate corrections during the integration process. This is the principle underlying multiple shooting methods. In multiple shooting, the interval $[t_0, t_\mathrm{f}]$ is partitioned into smaller subintervals. An initial value problem is solved independently on each subinterval, and the resulting partial trajectories are subsequently coupled by enforcing continuity (matching) conditions at the subinterval boundaries. This way, a solution over the entire interval $[t_0, t_\mathrm{f}]$ is constructed while improving numerical robustness. Multiple shooting is used in Papers A and C.

The distinction between single and multiple shooting can be clarified by the following analogy. Suppose an individual is asked to clap exactly once per second. As an initial reference, the individual hears the ticking of a clock for five seconds. If no further auditory cues are provided, maintaining the correct rhythm relies solely on the initial reference; any deviation will accumulate over time. This situation is analogous to single shooting, where the solution depends entirely on information specified at the initial time. Alternatively, assume that the individual hears two clock ticks every ten seconds as periodic reminders of the intended rhythm. These intermittent corrections help prevent the accumulation of timing errors. This scenario resembles multiple shooting, in which intermediate constraints provide corrective feedback during the solution process.

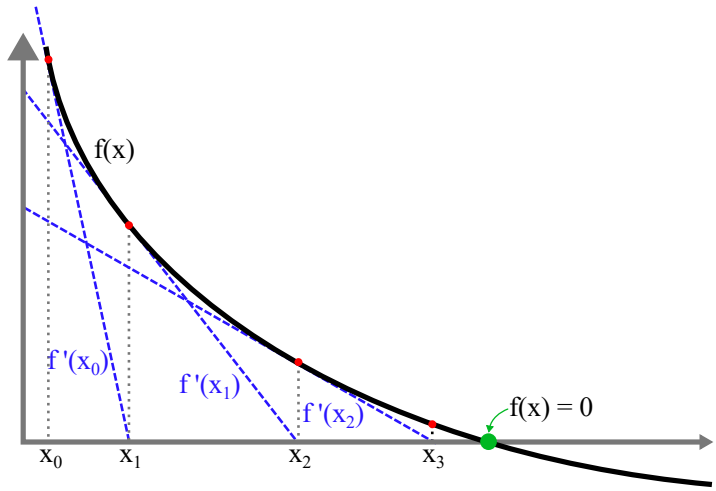

Figure 3.2: Illustration of how the Newton-Raphson method is used to find a root of function $f(x)$.

3.3 Newton-Raphson method

As mentioned in section 3.2, using the shooting method essentially translates into a root-finding problem, which has been solved numerically in Paper B with Newton-Raphson method (NRM), a common root-finding algorithm. The method is illustrated in Figure 3.2, where the root (green dot) of function $f(x)$ (gray line), is iteratively found by evaluating the derivative of the function at different points, starting from some x_0. The core idea behind the method is that if the function f satisfies certain conditions and if the initial guess x_0 is sufficiently close to its root, then every iteration of the method produces a better approximation of said root. This can be seen in Figure 3.2, as every iteration produces a solution that is closer to the root of the function.

The method used in Paper B is actually an approximated version of the NRM, since the derivatives of the function (i.e. the blue dashed lines in Figure 3.2) are not computed analytically but numerically, considering small variations of the variable x (i.e. Δx) and the corresponding variation of the

function $f(x)$ (i.e. Δf)

$$\frac{\mathrm{d}f}{\mathrm{d}x} \approx \frac{\Delta f}{\Delta x}. \tag{3.4}$$

3.4 Relaxation of binary variables

The OCPs described in (2.8) and (2.15) contain binary variables (vector $\mathbf{b}$). Binary variables often simplify the modeling of aspects which are inherently binary. In the case of this thesis, the choice of whether to charge the vehicle in a certain station. However, this makes the problem a mixed-integer one (binary variables are a subset of integer variables), which is usually computationally hard to solve. This is because such problems are often solved using a technique known as Branch-and-Bound [41], which essentially consists in enumerating the different possible combinations of values of the integer variables and checking which combination leads to the optimal solution. This guarantees that a global optimum is found, but it also makes the complexity of these algorithms grow exponentially with the size of the problem. Because of this, the discrete variables in Paper A are relaxed into continuous ones, so that a continuous solver can be used. However, this is an approximation of the original problem, and it is therefore important to ensure that the solution found through relaxation of the discrete variables is feasible for the original problem as well.

The discrete variables in the ICTP problem solved in Paper A are, more specifically, binary, and there is one associated to every charging station along the way. Let us define b_i as the binary variable associated to charging station i. Then, $b_i \in \{0, 1\}$, and $b_i = 1$ means that the planner has chosen station i to recharge the EV. To relax binary variables, it is sufficient to impose some additional inequality constraints in the problem. If b_i^r is the relaxed binary variable associated to charging station i, then the constraints are as follows

$$b_i^r \in [0, 1], \qquad i = 1, \ldots, N_\mathrm{b} \tag{3.5a}$$

$$b_i^r \cdot (1 - b_i^r) \leq \epsilon_i, \qquad i = 1, \ldots, N_\mathrm{b} \tag{3.5b}$$

$$\epsilon_i \geq 0, \qquad i = 1, \ldots, N_\mathrm{b} \tag{3.5c}$$

where $\epsilon^i \in \mathbb{R}$ is a slack variable for charging station i and N_c is the number of charging stations along the path. Additionally, for these constraints to work as intended, ϵ_i has to be minimized. To do that, an additional term is added

to the original cost function J of the OCP

$$J_{\text{relax}} = J + \rho \sum_{i=1}^{N_c} \epsilon_i \tag{3.6}$$

where ρ is a penalty term used to tune the weight of this additional term in the cost function.

To illustrate how this works, consider an example in which $\epsilon_i = 0.1$. Then, even though (3.5a) allows b_i^r to take on any value in $[0, 1]$, (3.5b) only holds if $b_i^r > 0.88 \vee b_i^r < 0.12$. It is then clear that the lower ϵ_i is, the closer b_i^r will be to either 0 or 1.

Notice that if $\epsilon = 0$, then the problem is not relaxed, but is rather a smooth reformulation of the original integer problem. However, while mixed-integer solvers would find the global optimum in the integer variables, the solution for the smooth reformulation might get trapped in a local optimum, depending on how the variables are initialized.

3.5 Interior point method

The interior point method [42] is a well-established algorithm to solve convex optimization problems. In this thesis, it has been used to solve the discretized optimal control problem in (2.15), following the relaxation of the binary variables described in Section 3.4. The OCPs presented in Papers A and C were solved using IPOPT, a numerical optimization solver based on the interior point method. In Paper B, the same solver was used to compute a benchmark solution, which was subsequently compared to the solution obtained using a method derived from Pontryagin's Maximum Principle.

The fundamental idea underlying interior point methods is to convert a constrained convex optimization problem into a sequence of unconstrained problems by introducing so-called barrier functions. These functions are constructed such that they tend to infinity as the solution approaches the boundary of the feasible set. By augmenting the original cost function with a barrier term, the constraints are implicitly enforced: although the reformulated problem is formally unconstrained, any minimization algorithm applied to the augmented objective will avoid the boundary of the feasible region, since doing so would cause the objective value to diverge. These barrier functions are progressively tightened, so that the barrier becomes increasingly steep near

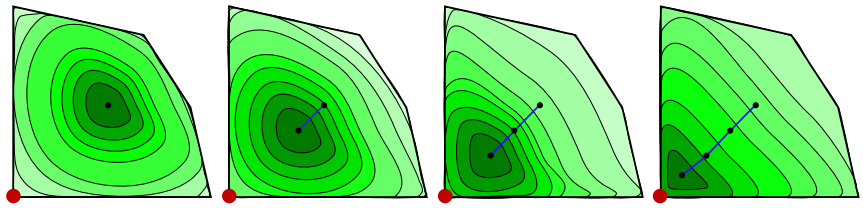

Figure 3.3: Illustration of how the barrier functions in the interior point method get steeper at every iteration, leading to the method converging to the real optimum of the problem.

the boundary. Consequently, the solution of each successive subproblem lies closer to the true constrained optimum. This procedure generates a sequence of solutions that follow a trajectory within the interior of the feasible region, commonly referred to as the central path, thereby giving the interior point method its name.

Figure 3.3 provides a schematic illustration of the interior point method over multiple iterations. The depicted region corresponds to the feasible set of the optimization problem, while the color map represents the value of the objective function, with darker shades indicating lower cost values. At each iteration, the barrier functions are tightened, which allows the solution to move closer to the boundary of the feasible region while remaining strictly feasible. As a result, the solution found at every iteration progressively converges toward the optimal solution of the original constrained problem (indicated by the red point in the lower left corner of the feasible set).

3.6 Pontryagin's maximum principle

In Paper B, explicit control laws for the the OCP in (2.8) are derived using Pontryagin's Maximum Principle (PMP), a core result in optimal control theory formulated in 1956 by Lev Pontryagin. The principle is used to find the optimal control for taking a dynamical system from one state to another. When used for minimization problems, it is usually referred to as Pontryagin's minimum principle.

The core concept behind PMP is the Hamiltonian function, which, given

an OCP formulated as (2.8), can be constructed as

$$H(\mathbf{x}, \mathbf{u}, \boldsymbol{\lambda}) = S(\mathbf{x}, \mathbf{u}) + \boldsymbol{\lambda}^{\mathrm{T}} \cdot f_x(\mathbf{x}, \mathbf{u}) \tag{3.7}$$

where $\boldsymbol{\lambda}$ is the vector of Lagrange multipliers (also called costates or dual variables), whose evolution over time is given by

$$\dot{\boldsymbol{\lambda}}(t) = -\frac{\partial H(\mathbf{x}, \mathbf{u}, \boldsymbol{\lambda})}{\partial \mathbf{x}(t)}. \tag{3.8}$$

These costates are those introduced in the extended state vector $\boldsymbol{\xi}$ in Section 3.1.

For a minimization problem, Pontryagin's minimum principle states that the optimal state trajectory $\mathbf{x}^*$, the optimal control vector $\mathbf{u}^*$, and the corresponding vector of optimal Lagrange multipliers $\boldsymbol{\lambda}^*$ must minimize the Hamiltonian H. That is

$$H(\mathbf{x}^*, \mathbf{u}^*, \boldsymbol{\lambda}^*) \leq H(\mathbf{x}, \mathbf{u}, \boldsymbol{\lambda}),\ \forall t \in [0, t_{\mathrm{f}}]. \tag{3.9}$$

Additionally, some boundary conditions need to hold for the solution to be optimal. These conditions depend on whether the final state $\mathbf{x}(t_{\mathrm{f}})$ and the final time t_{f} are fixed. The final state $\mathbf{x}(t_{\mathrm{f}})$ not being fixed results in the condition

$$\boldsymbol{\lambda}^{\mathrm{T}}(t_{\mathrm{f}}) = \frac{\partial \Psi(x(t_{\mathrm{f}}))}{\partial x} \tag{3.10}$$

while the final time t_{f} not being fixed results in the condition

$$\frac{\partial \Psi(x(t_{\mathrm{f}}))}{\partial t_{\mathrm{f}}} + H(t_{\mathrm{f}}) = 0. \tag{3.11}$$

The reason this principle is widely regarded as a milestone in optimal control theory is that minimizing (or maximizing) the Hamiltonian is, in general, much easier than solving the original OCP. This is because in the original OCP, the optimal control trajectories are found among an infinite number of curves. On the other hand, PMP aims at minimizing (or maximizing) the Hamiltonian at every time instant, meaning that, instead of finding the whole control trajectory at once, one finds the best value at a given time, then the best one at the next time instant and so on. This can be formally summarized by saying that PMP turns an infinite-dimensional OCP into a pointwise optimization.

CHAPTER 4

Assembling the blocks: trip-planning and speed optimization for EVs

This chapter illustrates how the elements presented in Chapters 2 and 3 are combined to answer the research questions listed in Section 1.3.

4.1 Computationally feasible solver for ICTP

In Paper A, the ICTP problem was formulated as a mixed-integer OCP, following the structure described in Section 2.2. The objective is to optimize the energy profile of an EV during a long-distance trip. Specifically, the optimal solution is required to

- minimize the vehicle's energy consumption while driving,
- determine the optimal selection of charging stations along the route, and
- optimize the charging process with respect to both charging time and economic cost. This is shown in Figure 4.2, where the cost function and each of its terms are defined. The variable c_i is the binary variable associated with the i^{th} charger along the trip, and is therefore one of the

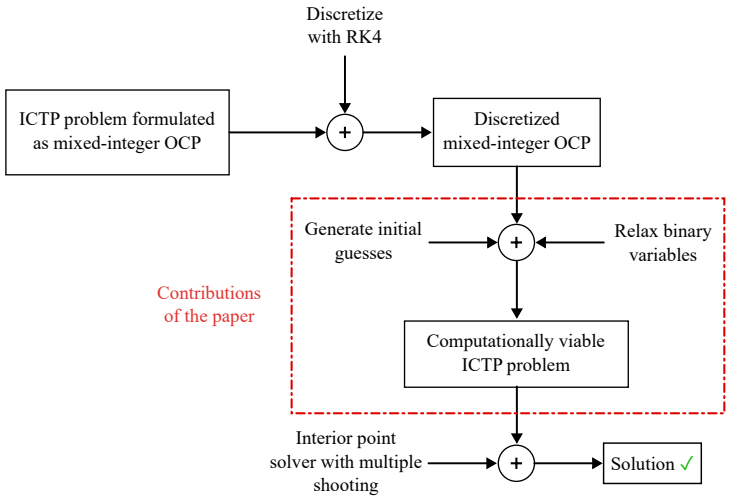

Figure 4.1: Schematic of the contributions of Paper A, where the ICTP problem was made more computationally feasible.

variables that is relaxed into a continuous one, according to Section 3.4. Notice that the integration variable in the last term of the cost function is τ_i, which is the elapsed time while charging at station i.

The controlled system is a vehicle modeled as a dynamical system with two states: a thermal state representing the battery temperature and an electrical state representing the SoC. The modeling of the thermal and electrical dynamics follows the description provided in Section 2.1. For numerical implementation, the continuous-time problem was discretized using an RK4 scheme, as detailed in Section 2.3, resulting in a formulation consistent with Section 2.4. The complete mathematical formulation of the OCP is presented in Paper A.

Due to its large scale, nonlinear dynamics, and mixed-integer structure, the resulting problem is computationally demanding, and the primary contribution of Paper A consists of reducing the problem's computational burden. The mixed-integer nature of the problem was first addressed by relaxing the binary decision variables, as described in Section 3.4. Subsequently, a heuris-

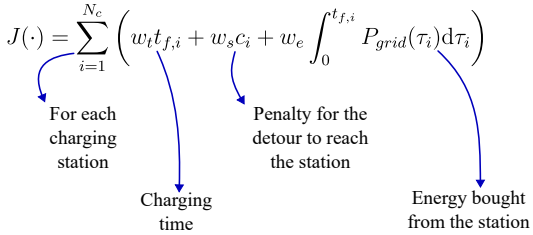

Figure 4.2: Cost function minimized in the OCP in Paper A.

Figure 4.3: Visualization of the ICTP problem as a trip between Gothenburg and Stockholm, with two alternatives to recharge along the way (yellow).

tic algorithm was developed to generate initial guesses in the vicinity of the optimal solution, thereby performing an effective warm start of the solver. An example of a guess generated by the algorithm, compared with the optimal solution, is shown in Figure 4.4. The combination of binary relaxation and informed initialization significantly improved computational tractability. In particular, the problem could be efficiently solved using a multiple shooting approach in conjunction with an interior-point method, as outlined in Sections

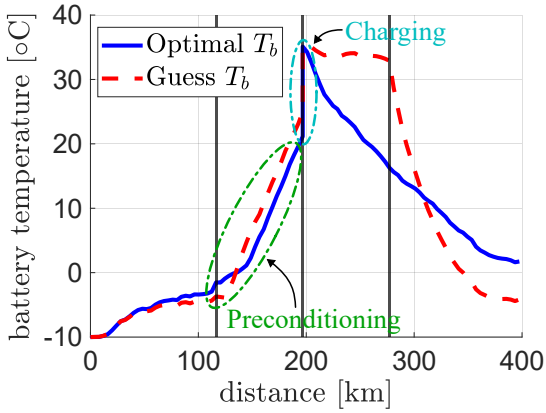

Figure 4.4: Example of comparison between optimal and guessed trajectory for T_{b}.

3.2 and 3.5. This approach achieved an average execution time reduction of approximately 91.07%, while inducing only a negligible increase in average driving energy consumption. A schematic overview of the overall methodology is provided in Figure 4.1.

An illustrative example is shown in Fig. 4.3, representing a trip between Gothenburg and Stockholm. Two candidate charging locations, Örebro and Jönköping, are highlighted as alternative recharging options. The charger selection problem thus corresponds to selecting one of the two possible routes. In this context, the binary decision variables are associated with the charging stations in Örebro and Jönköping. For example, if the binary variable corresponding to Örebro is equal to 1, the charging station in Örebro is selected and the upper route is chosen by the solver.

4.2 Semi-analytical solution for the charging OCP

In Paper B, the charging optimization problem was formulated as an OCP, following the structure described in Section 2.2. The goal of the charging optimization problem is to recharge the battery to a desired level of SoC, while minimizing a trade-off between the charging time t_{f} and the economic cost (represented by the energy bought from the grid). The cost function to

be minimized is, therefore,

$$J(\cdot) = w_{\mathrm{t}} t_{\mathrm{f}} + w_{\mathrm{e}} \int_0^{t_{\mathrm{f}}} P_{\mathrm{grid}}(\cdot) dt \tag{4.1}$$

where w_{t} and w_{e} are, respectively, the weights for charging time and for economic cost, and P_{grid} is the power bought from the grid. Tuning w_{t} and w_{e} allows one to manage the trade-off between the two terms of the cost function. For instance, if the driver is in a hurry and, therefore, cares more about charging fast than about the charging process being cheap, then w_{t} and w_{e} should be chosen such that the first term is more relevant than the second.

The continuous-time problem was discretized using an RK4 scheme, as presented in Section 2.3, resulting in a discrete OCP formulation consistent with Section 2.4. The vehicle model employed in the OCP is essentially identical to that used in Paper A (see Section 4.1). The main objective of the study was to solve the OCP using a single shooting approach, as described in Section 3.2, based on Pontryagin's Maximum Principle (PMP).

As outlined in Section 3.6, solving an OCP using PMP requires minimizing the Hamiltonian H (defined in (3.7)) while enforcing some optimality conditions. In this specific problem, the optimality conditions are given by

$$\mathrm{SoC}(t_{\mathrm{f}}) = \mathrm{SoC}_{\mathrm{des}}, \tag{4.2a}$$

$$\lambda_{T_{\mathrm{b}}}(t_{\mathrm{f}}) - \frac{\partial \Psi^*(t_{\mathrm{f}})}{\partial x} = 0, \tag{4.2b}$$

$$H^*(t_{\mathrm{f}}) + \frac{\partial \Psi^*(t_{\mathrm{f}})}{\partial t_{\mathrm{f}}} = 0. \tag{4.2c}$$

Equation (4.2a) enforces the terminal constraint that the final SoC at the end of the charging process equals the desired value. Condition (4.2b) arises from the fact that the final battery temperature $T_{\mathrm{b}}(t_{\mathrm{f}})$ is free, whereas (4.2c) follows from the final charging time being free.

Conceptually, the solution procedure consists of initializing the states $\mathbf{x}(0)$ and costates $\boldsymbol{\lambda}(0)$, and simulating the charging process over the interval $[0, t_{\mathrm{f}}]$, while selecting control inputs that minimize the Hamiltonian. The resulting control inputs are used to propagate both states and costates forward in time, with the costates evolving according to (3.8). At the end of the charging horizon, the optimality conditions in (4.2) are evaluated. However, although the initial state $\mathbf{x}(0)$ is known, the initial costates $\boldsymbol{\lambda}(0)$ are not. In addition,

the terminal time t_f is a decision variable to be minimized and is therefore also unknown. Moreover, whether the optimality conditions in (4.2) are satisfied or not depends on $\boldsymbol{\lambda}(0)$ and t_f. This procedure needs to therefore be corrected by taking into account the fact that $\boldsymbol{\lambda}(0)$ and t_f are unknown and need to be computed. A high-level description of the implemented algorithm

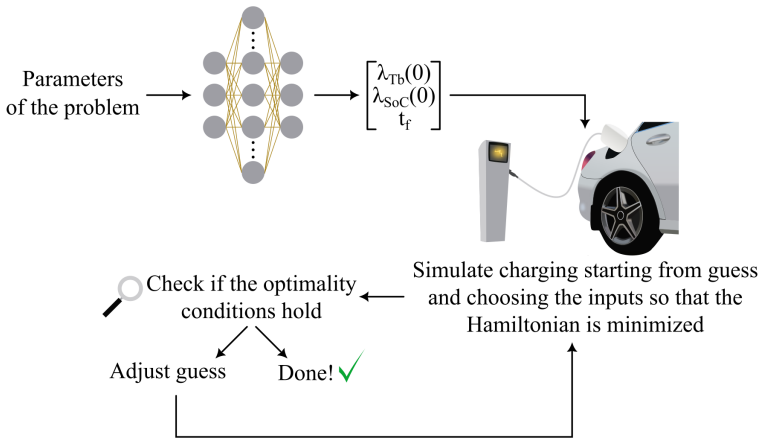

Figure 4.5: High-level view of the algorithm used in Paper B to solve the charging OCP with a PMP-based solver.

is provided in Figure 4.5. The known parameters of the problem, such as the initial states and the desired SoC, are provided as inputs to a neural network designed to generate an initial estimate of the unknown quantities $\boldsymbol{\lambda}(0)$ and t_f. Given these estimates, the charging process is simulated by minimizing the Hamiltonian at each time step. After completion of the simulation, the optimality conditions are evaluated. If they are satisfied, the OCP is considered solved, since minimizing the Hamiltonian subject to the PMP conditions is equivalent to solving the original problem. If the conditions are not satisfied, the estimates of $\boldsymbol{\lambda}(0)$ and t_f are updated and the simulation is repeated.

The iterative update of the unknown initial costates and terminal time corresponds to solving a nonlinear system of equations. In Paper B, this task is carried out using an approximated version of the Newton–Raphson method, as described in Section 3.3. The approach is classified as a single shooting

method, as discussed in Section 3.2, because the correctness of the computed trajectory is assessed only at the end of its calculation (i.e. without intermediate checks). If the terminal conditions are not met, the entire trajectory is recomputed at the subsequent iteration.

This framework enables the solution of the OCP without relying on external optimization solvers, which is advantageous for potential implementation on embedded hardware platforms.

4.3 Solar-powered vehicle racing

Figure 4.6: Path of the BWSC and the two kinds of stops considered in Paper C.

Paper C considers a nonlinear minimum-time OCP for long-distance mission planning of a solar-powered electric vehicle competing in the Bridgestone World Solar Challenge (BWSC). Section 2.1 provides a schematic of the sources of solar energy considered in the paper, as well as a diagram of the forces acting on the vehicle. The BWSC consists of a 3022 km race across the Australian Outback, from Darwin to Adelaide. Since propulsion relies exclusively on solar energy, completing the race is challenging and requires efficient energy management, and achieving this objective in minimum time further increases the level of difficulty. In addition to optimal energy management, several spatio-temporal constraints must be satisfied in accordance with the official competition rules, including mandatory stops.

Along the route, checkpoints must be reached within prescribed time windows to avoid disqualification. Upon arrival at a checkpoint, the vehicle is required to stop for 30 minutes, during which charging is permitted. Although the arrival time at each checkpoint is not known a priori, the checkpoint locations are fixed. These stops are therefore classified as location-triggered stops (LTS). Moreover, the vehicle is allowed to drive only between 08:00 and 17:00. The exact location of the vehicle at the start of the mandatory overnight stop is not known in advance; however, the stopping time is predetermined. These stops are therefore referred to as time-triggered stops (TTS).

The system dynamics differ depending on whether the vehicle is driving or charging. When a stop begins, the dynamic model must switch from driving dynamics to charging dynamics, and vice versa once driving resumes. A natural modeling approach is to introduce a binary variable to represent this mode switch. However, as previously discussed, avoiding binary variables is preferable due to the associated increase in computational complexity.

The choice of modeling domain, time or space, favors one class of stops over the other. If the OCP is formulated in time domain, TTS events are straightforward to model because their occurrence times are known and can be explicitly incorporated into the problem formulation. In this case, however, the vehicle position becomes a decision variable, implying that LTS events depend on state values that are determined only after solving the OCP. Conversely, if the problem is formulated in the spatial domain, LTS events can be more naturally represented, while TTS events become more challenging to handle. This trade-off represents only one of several modeling challenges inherent to the problem. A high-level overview of the main modeling issues is provided in Fig. 4.7, while a detailed treatment can be found in Paper C.

One of the state variables of the OCP is driving time τ, which varies according to

$$\frac{\mathrm{d}\tau(t)}{\mathrm{d}t} = \begin{cases} 1, & \text{if } t \notin \mathbb{T}_{\text{stop}} \text{ and } s(t) \notin \mathbb{S}_{\text{stop}} \\ 0, & \text{otherwise} \end{cases} \tag{4.3}$$

where $\mathbb{T}_{\text{stop}}$ and $\mathbb{S}_{\text{stop}}$ are, respectively, the sets of the times and locations for the TTS and the LTS (assumed to be known in advance). Essentially, τ only varies when the EV is moving. Piecewise-defined equations introduce potential non-differentiabilities if not treated carefully. Such formulations effectively correspond to conditional (if–else) statements. For example, if the vehicle is driving, the elapsed driving time τ should increase; otherwise, it

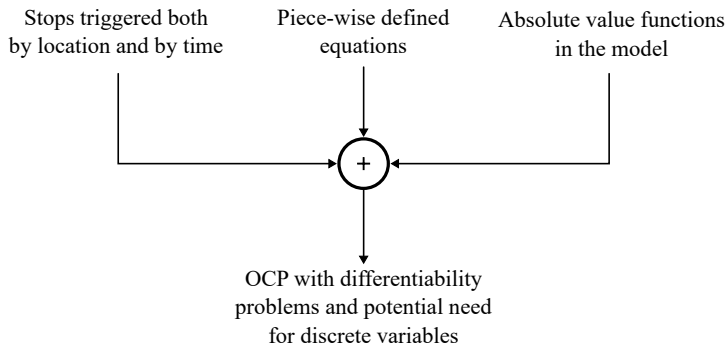

Figure 4.7: Diagram showing the modeling issues of the OCP solved in Paper C.

should remain constant. A direct implementation of this logic would require a binary variable indicating whether the EV is in motion, thereby introducing discrete decision variables into the problem. Another state variable is the kinetic energy E_{k}, which depends on the acceleration a. If the powertrain efficiency differs between traction ($a > 0$) and regenerative braking ($a < 0$), the dynamic equation governing E_{k} would also require a piecewise definition to distinguish between these operating regimes. Finally, the aerodynamic drag is defined as

$$F_{\mathrm{drag}}(E_{\mathrm{k}}) = \frac{1}{2}\rho_{\mathrm{air}} c_{\mathrm{D}} A_{\mathrm{f}} v_{\mathrm{rel}}(E_{\mathrm{k}}) |v_{\mathrm{rel}}(E_{\mathrm{k}})|. \tag{4.4}$$

where ρ_{air} is the air density, c_{D} is the drag coefficient, A_{f} is the vehicle's frontal area and v_{rel} is the relative velocity of the vehicle with respect to the apparent wind along its path. The presence of the absolute value operator introduces a point of nondifferentiability at zero relative velocity. The main contribution of Paper C is to address all the above-mentioned issues without the use of binary variables, in order to preserve differentiability and to allow the use of continuous solvers.

The OCP was formulated in the spatial domain, thereby favoring the modeling of LTSs. In the original time-domain formulation, both the driving time and the vehicle position appear as state variables. Since the driving time is a decision variable to be minimized, it must remain in the formulation. On the other hand, the vehicle position can be eliminated as a state variable by

adopting a space-domain representation. This reformulation reduces therefore the overall problem dimension.

To avoid a piecewise definition of the kinetic energy dynamics with respect to the sign of the acceleration a, the acceleration was decomposed into two components: a^+ (traction, positive) and a^- (braking, negative), such that

$$a = a^+ + a^- \tag{4.5}$$

This decomposition is valid provided that both components are not simultaneously nonzero, but that would not happen, as it would correspond to concurrent traction and braking, which is energetically inefficient. Since the objective is minimum-time performance under energy constraints, the optimal solution provides no incentive for such behavior, making the decomposition valid.

To address the non-differentiability introduced by the absolute value in the aerodynamic drag expression F_{drag}, the drag force is defined as a dummy control input and its original definition in (4.4) is replaced by the pair of inequality constraints

$$F_{\text{drag}}(s) \geq \frac{1}{2}\rho_{\text{air}} c_{\text{D}} A_{\text{f}} v_{\text{rel}}^2(E_{\text{k}}) \tag{4.6a}$$

$$F_{\text{drag}}(s) \geq -\frac{1}{2}\rho_{\text{air}} c_{\text{D}} A_{\text{f}} v_{\text{rel}}^2(E_{\text{k}}). \tag{4.6b}$$

Although this formulation appears to be a relaxation of the original equality constraint in (4.4), it yields an exact representation at the optimum. In fact, depending on the sign of v_{rel}, one of the two inequalities becomes active and holds with equality, leading effectively to

$$F_{\text{drag}}^*(s) = \begin{cases} \frac{1}{2}\rho_{\text{air}} c_{\text{D}} A_{\text{f}} v_{\text{rel}}^2(E_{\text{k}}^*), & \text{if } v_{\text{rel}} \geq 0 \\ -\frac{1}{2}\rho_{\text{air}} c_{\text{D}} A_{\text{f}} v_{\text{rel}}^2(E_{\text{k}}^*), & \text{if } v_{\text{rel}} < 0. \end{cases} \tag{4.7}$$

If neither inequality were active, the drag force would exceed its physically required value, resulting in unnecessary energy expenditure. Such behavior would be suboptimal and therefore avoided by the solver. It is important to notice that (4.7) is not explicitly implemented in the OCP, as this would reintroduce a piecewise definition and potentially require integer variables. Instead, (4.7) is simply a representation of how the auxiliary control formulation ensures that the appropriate value of F_{drag} is selected implicitly through the optimization process.

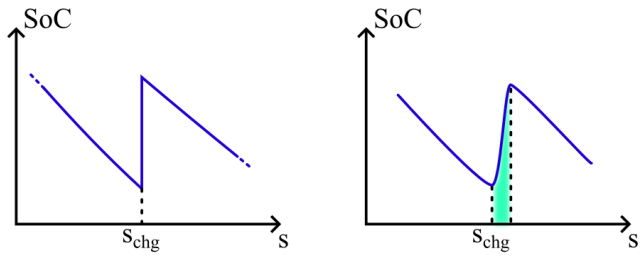

Figure 4.8: Visualization of how the charging process during a stop is smoothened in Paper C.

Formulating the OCP in the spatial domain reduces the problem dimension, but it introduces challenges related to charging. The vehicle can recharge both while driving and while stationary during mandatory stops. The latter case requires particular attention. When charging occurs while the vehicle is stationary, the spatial coordinate remains constant, and the corresponding increase in SoC appears concentrated within a single spatial sample. In a space-domain formulation, this manifests as a vertical jump in the SoC trajectory, analogous to a Dirac impulse, which leads to differentiability issues.

Such behavior would not arise in a time-domain formulation, where the charging process is naturally distributed over a finite time interval. Furthermore, since the problem is discretized in space, the differentiability issue primarily affects time-triggered stops (TTS). For location-triggered stops (LTS), the stopping positions are known a priori, and the associated impulse-like changes in SoC can be directly integrated, resulting in a discrete increment ΔSoC applied at a known spatial point.

The approach proposed in Paper C consists of smoothening the impulse-like behavior by distributing the charging process over a small spatial interval rather than a single spatial sample. This concept is illustrated in Figure 4.8. In the idealized representation (left plot of Figure 4.8), the SoC increases instantaneously at a single spatial point, which causes differentiability problems. In the smoothed formulation (right plot of Figure 4.8), the same energy increment is spread over a short spatial segment, yielding a differentiable approximation. The length of this spatial interval introduces a trade-off: a shorter interval improves fidelity with respect to the physical process but increases the risk of numerical difficulties associated with steep gradients.

Due to the overall complexity of the problem, discretization was performed using the forward Euler method, as described in Section 2.3, since the use of an RK4 scheme resulted in feasibility issues. The resulting discrete OCP was solved using a multiple shooting strategy combined with an interior-point method, as detailed in Sections 3.2 and 3.5. The computed driving profile was closely followed during the race, and the vehicle completed the competition in a time comparable to the simulation-based prediction.

Although the primary application in Paper C concerns a racing scenario, the proposed methodology is applicable to other mission-planning problems with similar structural characteristics. For example, in a minimum-time routing problem for a freight vehicle, LTSs could represent delivery locations, while TTSs could correspond to legally mandated rest periods after a prescribed driving duration. In such a case, the specific propulsion system would modify the physical modeling of the vehicle but would not fundamentally alter the structure of the optimal control formulation.

CHAPTER 5

Summary of included papers

This chapter provides a summary of the included papers.

5.1 Paper A

Lorenzo Montalto, Nikolce Murgovski, Jonas Fredriksson
Computationally efficient algorithm for optimal battery preconditioning and charging of electric vehicles
2024 IEEE 27th International Conference on Intelligent Transportation Systems (ITSC), Edmonton, AB, Canada, 2024, pp. 1600-1605, doi: 10.1109/ITSC58415.2024.10920033.
© 2024 IEEE. Reprinted with permission, from 2024 IEEE 27th International Conference on Intelligent Transportation Systems (ITSC), Edmonton, AB, Canada, 2024.

This paper aims at improving the computational availability of the ICTP problem, which is large-scale, nonlinear and mixed-integer. This was achieved through an algorithm which generates initial guesses close to the optimum, to warm-start the solver. Moreover, the mixed-integer problem was converted to

a continuous one by relaxing its binary variables, so that it could be solved with a much faster continuous solver. This led to an average reduction in computation time of about 91%

Contributions: LM contributed to the software implementation and its validation, and wrote the original draft. NM contributed to the original conceptualization and provided supervision during implementation and writing. JF provided supervision during implementation and writing.

5.2 Paper B

> **Lorenzo Montalto**, Nikolce Murgovski, Jonas Fredriksson
> Electrical vehicles charging: an optimal control approach via Pontryagin's Maximum Principle
> *2025 IEEE 28th International Conference on Intelligent Transportation Systems (ITSC)*, Gold Coast, QLD, Australia, 2025, to appear in conference proceedings.

This article develops a semi-analytical solver to the charging optimization problem for EVs. The solver is based on Pontryagin's Maximum Principle, which allows the derivation of explicit expressions for the optimal control trajectories. The developed solver has comparable computational performance with an off-the-shelf one used as benchmark and the solution is more interpretable and easier to implement on integrated hardware thanks to its independence from external solvers.

Contributions: LM contributed to the software implementation and its validation, and wrote the original draft. NM contributed to the original conceptualization and provided supervision during implementation and writing. JF provided supervision during implementation and writing.

5.3 Paper C

> **Lorenzo Montalto**, Nikolce Murgovski, Timothy Jarebrant
> Optimal energy management under spatio-temporal constraints: an application to solar-powered vehicles
> Under review in *Control Engineering Practice*, Elsevier, 2026.

This article addresses a nonlinear OCP for mission planning of long-range

solar-powered EVs. The goal is to optimize trip time and energy management while guaranteeing differentiability, computational efficiency and compliance with given spatio-temporal constraints. The method was tested on a vehicle competing in the Bridgestone World Solar Challenge, a 3 022 km race across the Australian Outback.

Contributions: LM provided supervision during implementation, contributed to validation and wrote the original draft. NM contributed to the original conceptualization, to the software implementation and its validation and provided supervision during implementation and writing. TJ contributed to the original conceptualization, validated the software on the analyzed case study and contributed to writing.

CHAPTER 6

Concluding Remarks and Future Work

6.1 Conclusions

The transport sector is widely recognized as a major contributor to global warming, which has led to increasingly stringent environmental legislation worldwide. A central pillar of the transition toward more sustainable mobility solutions is the widespread adoption of EVs, particularly when combined with low-carbon electricity generation. However, despite technological progress, range anxiety remains a major factor that discourages EV adoption. One approach to address range-anxiety is ICTP, which consists of solving a combined optimization problem involving the optimization of the selection of charging stations, the battery thermal management and the vehicle's energy consumption along the route, and the charging process itself, in terms of both charging time and economic cost.

This thesis addresses the development of computationally feasible and real-time implementable solution methods for the ICTP problem. Given the large-scale, nonlinear and mixed-integer nature of ICTP formulations, achieving both numerical robustness and practical deployability poses significant challenges. The research presented in this work contributes to algorithmic and

analytical advances that reduce computational burden while preserving solution quality and interpretability.

Paper A focuses on improving the computational tractability of the ICTP problem. Due to its large-scale, nonlinear, and mixed-integer structure, direct solution using standard optimization solvers can be time-consuming. To address this, an algorithm was developed to generate high-quality initial guesses close to the optimal solution, enabling effective warm-starting of the solver. In addition, the original mixed-integer formulation was reformulated by relaxing the binary decision variables, thereby transforming the problem into a continuous one that can be handled by significantly faster continuous solvers. This combined strategy resulted in an average reduction in computation time of approximately 91%.

Paper B develops a semi-analytical solver for the charging optimization problem of electric vehicles. The approach is based on Pontryagin's Maximum Principle, which enables the derivation of explicit expressions for the optimal control trajectories. By exploiting the structure of the problem, the proposed solver achieves computational performance comparable to that of a benchmark off-the-shelf numerical solver. At the same time, the resulting solution structure is more interpretable and particularly well suited for embedded implementation, as it does not rely on external numerical optimization software, facilitating integration into onboard hardware.

Paper C addresses a nonlinear optimal control problem for the mission planning problem of long-range solar-powered electric vehicles. The objective is to jointly optimize trip time and energy management while ensuring differentiability, computational efficiency, and compliance with prescribed spatio-temporal constraints. The proposed method was validated on a vehicle competing in the Bridgestone World Solar Challenge, a 3,022 km race across the Australian Outback. Following the driving profile computed by the method, the vehicle was able to complete the race.

Overall, these contributions show how optimal control methods can be used to solve the ICTP problem while ensuring both computational availability and real-time implementability, essentially providing a software-side solution to range anxiety.

6.2 Future work

The research presented in this thesis opens several promising directions for future work. A first natural extension concerns the generalization of the PMP-based solver developed in Paper B. The current implementation, which addresses the charging optimization problem, could be extended to the driving phase, i.e., the problem of optimally driving to a charging station while ensuring optimal BTM and energy consumption. The ultimate objective is to develop a unified PMP-based solver to handle the entire ICTP problem, including driving, charging station selection, and charging. In this context, the heuristic algorithm introduced in Paper A for generating initial guesses could be used to initialize the solver, thus improving convergence and robustness.

Another important research direction concerns the incorporation of stochastic information related to charging station availability. Historical usage data from charging infrastructure could be used to construct probabilistic models that predict charger occupancy as a function of location, day, and time of day. Integrating such models into the ICTP framework would enable a more informed charging station selection process, particularly in scenarios where congestion at charging stations significantly affects travel time.

The integration of user preferences represents an additional avenue for development. The current framework already allows weighting different objectives, such as charging time versus economic cost. Future work could expand this personalization aspect to include preferences related to charging station selection, such as proximity to specific amenities (e.g., restaurants or services), preferred charging times, and other such factors.

Further validation of the proposed algorithms using real-world datasets obtained from industrial partners is also essential to validate model accuracy, computational performance, and robustness. Such validation would also facilitate the identification of modeling gaps and practical constraints that may not be fully captured in simulation-based studies.

Finally, a methodological shift toward reinforcement learning (RL) or approximated DP approaches constitutes a longer-term research direction. While the current work relies primarily on model-based optimal control techniques, RL and DP offer alternative frameworks that may better handle high-dimensional decision spaces, uncertainty, and long planning horizons. Hybrid approaches combining model-based optimal control with data-driven learning methods will also be considered.

References

[1] E. Commission, *European climate law*. [Online]. Available: https://climate.ec.europa.eu/eu-action/european-climate-law_en.

[2] U. Nations, *A beginner's guide to climate neutrality*. [Online]. Available: https://unfccc.int/news/a-beginner-s-guide-to-climate-neutrality.

[3] U. Nations, *The paris agreement*. [Online]. Available: https://unfccc.int/process-and-meetings/the-paris-agreement.

[4] C. C. C. Service, *Global climate highlights 2024*. [Online]. Available: https://climate.copernicus.eu/global-climate-highlights-2024.

[5] H. Ritchie, P. Rosado, and M. Roser, *Data page: CO_2 emissions from transport*, Data adapted from Climate Watch, 2023. [Online]. Available: https://ourworldindata.org/grapher/co2-emissions-transport.

[6] S. Sobczuk and A. Borucka, "Recent advances for the development of sustainable transport and their importance in case of global crises: A literature review," *Applied Sciences*, vol. 14, no. 22, 2024, ISSN: 2076-3417. [Online]. Available: https://www.mdpi.com/2076-3417/14/22/10653.

[7] J. Jaguemont, L. Boulon, P. Venet, Y. Dubé, and A. Sari, "Lithium-ion battery aging experiments at subzero temperatures and model development for capacity fade estimation," *IEEE Transactions on Vehicular Technology*, vol. 65, no. 6, pp. 4328–4343, 2016.

[8] R. Kish, "Are electric vehicles really green?" *Economic Affairs*, vol. 43, no. 2, 2023.

[9] N. Rauh, T. Franke, and J. F. Krems, "Understanding the impact of electric vehicle driving experience on range anxiety," *Human Factors*, vol. 57, no. 1, pp. 177–187, 2015, PMID: 25790577. [Online]. Available: https://doi.org/10.1177/0018720814546372.

[10] M. Ahmadi, N. Mithulananthan, and R. Sharma, "A review on topologies for fast charging stations for electric vehicles," in *2016 IEEE International Conference on Power System Technology (POWERCON)*, 2016, pp. 1–6.

[11] J. A. NeJame, "Examining the role of gender in electric vehicle interest and purchasing intention," M.S. thesis, The Ohio State University, 2024.

[12] M. Redelbach, E. D. Özdemir, and H. E. Friedrich, "Optimizing battery sizes of plug-in hybrid and extended range electric vehicles for different user types," *Energy Policy*, vol. 73, pp. 158–168, 2014, ISSN: 0301-4215. [Online]. Available: https://www.sciencedirect.com/science/article/pii/S030142151400367X.

[13] A. Dinc and M. Otkur, "Optimization of electric vehicle battery size and reduction ratio using genetic algorithm," in *2020 11th International Conference on Mechanical and Aerospace Engineering (ICMAE)*, 2020, pp. 281–285.

[14] C. Zhu, F. Lu, H. Zhang, and C. C. Mi, "Robust predictive battery thermal management strategy for connected and automated hybrid electric vehicles based on thermoelectric parameter uncertainty," *IEEE Journal of Emerging and Selected Topics in Power Electronics*, vol. 6, no. 4, pp. 1796–1805, 2018.

[15] Y. Huang, E. C. Ng, J. L. Zhou, N. C. Surawski, E. F. Chan, and G. Hong, "Eco-driving technology for sustainable road transport: A review," *Renewable and Sustainable Energy Reviews*, vol. 93, pp. 596–609, 2018, ISSN: 1364-0321. [Online]. Available: https://www.sciencedirect.com/science/article/pii/S1364032118303745.

[16] Z. Yi and P. H. Bauer, "Optimal stochastic eco-routing solutions for electric vehicles," *IEEE Transactions on Intelligent Transportation Systems*, vol. 19, no. 12, pp. 3807–3817, 2018.

[17] S. Pourazarm, C. G. Cassandras, and A. Malikopoulos, "Optimal routing of electric vehicles in networks with charging nodes: A dynamic programming approach," in *2014 IEEE International Electric Vehicle Conference (IEVC)*, 2014, pp. 1–7.

[18] L. Z. Velimirović, A. Janjić, P. Vranić, J. D. Velimirović, and I. Petkovski, "Determining the optimal route of electric vehicle using a hybrid algorithm based on fuzzy dynamic programming," *IEEE Transactions on Fuzzy Systems*, vol. 31, no. 2, pp. 609–618, 2022.

[19] Y. Zhang, W. Cao, H. Zhao, and S. Gao, "Route planning algorithm based on dynamic programming for electric vehicles delivering electric power to a region isolated from power grid," *Artificial Life and Robotics*, vol. 28, no. 3, pp. 583–590, 2023.

[20] B. Lin, B. Ghaddar, and J. Nathwani, "Deep reinforcement learning for the electric vehicle routing problem with time windows," *IEEE Transactions on Intelligent Transportation Systems*, vol. 23, no. 8, pp. 11 528–11 538, 2021.

[21] R. Basso, B. Kulcsár, I. Sanchez-Diaz, and X. Qu, "Dynamic stochastic electric vehicle routing with safe reinforcement learning," *Transportation research part E: logistics and transportation review*, vol. 157, p. 102 496, 2022.

[22] M. Tang, W. Zhuang, B. Li, H. Liu, Z. Song, and G. Yin, "Energy-optimal routing for electric vehicles using deep reinforcement learning with transformer," *Applied Energy*, vol. 350, p. 121 711, 2023.

[23] W. Tang and Y. J. Zhang, "A model predictive control approach for low-complexity electric vehicle charging scheduling: Optimality and scalability," *IEEE Transactions on Power Systems*, vol. 32, no. 2, pp. 1050–1063, 2017.

[24] A. Di Giorgio, F. Liberati, and S. Canale, "Electric vehicles charging control in a smart grid: A model predictive control approach," *Control Engineering Practice*, vol. 22, pp. 147–162, 2014.

[25] X. Zeng and J. Wang, "A parallel hybrid electric vehicle energy management strategy using stochastic model predictive control with road grade preview," *IEEE Transactions on Control Systems Technology*, vol. 23, no. 6, pp. 2416–2423, 2015.

[26] R. V. Gamkrelidze, "Discovery of the maximum principle," in *Mathematical events of the twentieth century*, Springer, 2006, pp. 85–99.

[27] S. Bauer, A. Suchaneck, and F. Puente León, "Thermal and energy battery management optimization in electric vehicles using pontryagin's maximum principle," *Journal of Power Sources*, vol. 246, pp. 808–818, 2014, ISSN: 0378-7753. [Online]. Available: https://www.sciencedirect.com/science/article/pii/S0378775313013591.

[28] R. Schmid, J. Buerger, and N. Bajcinca, "Energy management strategy for plug-in-hybrid electric vehicles based on predictive pmp," *IEEE Transactions on Control Systems Technology*, vol. 29, no. 6, pp. 2548–2560, 2021.

[29] M. Salazar, A. Houshmand, C. G. Cassandras, and M. Pavone, "Optimal routing and energy management strategies for plug-in hybrid electric vehicles," in *2019 IEEE Intelligent Transportation Systems Conference (ITSC)*, IEEE, 2019, pp. 733–739.

[30] T. J. Boehme, F. Held, C. Rollinger, H. Rabba, M. Schultalbers, and B. Lampe, "Application of an optimal control problem to a trip-based energy management for electric vehicles," *SAE International Journal of Alternative Powertrains*, vol. 2, no. 1, pp. 115–126, 2013, ISSN: 21674191, 21674205. Accessed: Feb. 12, 2026. [Online]. Available: http://www.jstor.org/stable/26167725.

[31] M. Vajedi, "Real-time optimal control of a plug-in hybrid electric vehicle using trip information," Ph.D. dissertation, University of Waterloo, 2016.

[32] H. Abbas, Y. Kim, J. B. Siegel, and D. M. Rizzo, "Synthesis of pontryagin's maximum principle analysis for speed profile optimization of all-electric vehicles," *Journal of Dynamic Systems, Measurement, and Control*, vol. 141, no. 7, p. 071 004, Mar. 2019, ISSN: 0022-0434. [Online]. Available: https://doi.org/10.1115/1.4043117.

[33] C. Hou, M. Ouyang, L. Xu, and H. Wang, "Approximate pontryagin's minimum principle applied to the energy management of plug-in hybrid electric vehicles," *Applied Energy*, vol. 115, pp. 174–189, 2014, ISSN: 0306-2619. [Online]. Available: https://www.sciencedirect.com/science/article/pii/S0306261913008945.

[34] Y. Ma, Q. Ma, Y. Liu, and J. Gao, "Adaptive optimization control strategy for electric vehicle battery thermal management system based on pontryagin's minimal principle," *IEEE Transactions on Transportation Electrification*, vol. 10, no. 2, pp. 3855–3869, 2024.

[35] Y. Tan, J. Mao, and K. Tseng, "Modelling of battery temperature effect on electrical characteristics of li-ion battery in hybrid electric vehicle," in *2011 IEEE Ninth International Conference on Power Electronics and Drive Systems*, 2011, pp. 637–642.

[36] M. Steinstraeter, T. Heinrich, and M. Lienkamp, "Effect of low temperature on electric vehicle range," *World Electric Vehicle Journal*, vol. 12, no. 3, 2021, ISSN: 2032-6653. [Online]. Available: `https://www.mdpi.com/2032-6653/12/3/115`.

[37] J. Lindgren and P. D. Lund, "Effect of extreme temperatures on battery charging and performance of electric vehicles," *Journal of Power Sources*, vol. 328, pp. 37–45, 2016, ISSN: 0378-7753. [Online]. Available: `https://www.sciencedirect.com/science/article/pii/S0378775316308941`.

[38] A. I. Ilies, R. Jánó, and A. Fodor, "Battery preconditioning methods for electric vehicles in cold climates: A comparative review," in *2025 International Spring Seminar on Electronics Technology (ISSE)*, 2025, pp. 1–7.

[39] Y. Li, L. Wang, C. Liao, L. Wu, J. Li, and Y. Guo, "Effects of temperature on dynamic characteristics of li-ion batteries in electric vehicle applications," in *2014 IEEE Conference and Expo Transportation Electrification Asia-Pacific (ITEC Asia-Pacific)*, 2014, pp. 1–6.

[40] S. Tong, M. P. Klein, and J. W. Park, "On-line optimization of battery open circuit voltage for improved state-of-charge and state-of-health estimation," *Journal of Power Sources*, vol. 293, pp. 416–428, 2015.

[41] S. Boyd and J. Mattingley, "Branch and bound methods," *Notes for EE364b, Stanford University*, vol. 2006, p. 07, 2007.

[42] F. A. Potra and S. J. Wright, "Interior-point methods," *Journal of Computational and Applied Mathematics*, vol. 124, no. 1, pp. 281–302, 2000, Numerical Analysis 2000. Vol. IV: Optimization and Nonlinear Equations, ISSN: 0377-0427.